Chinese Journal of Oceanology and Limnology
Vol. 33 No. 1, P. 176-193, 2015
http://dx.doi.org/10.1007/s00343-015-4061-6

Nutrient fluxes in the Changjiang River estuary and adjacent waters — a modified box model approach*

WANG Xiaohong (王晓红)[1, 2, 3], YU Zhiming (俞志明)[1, **], FAN Wei (樊伟)[4], SONG Xiuxian (宋秀贤)[1], CAO Xihua (曹西华)[1], YUAN Yongquan (袁涌铨)[1]

[1] *Key Laboratory of Marine Ecology and Environmental Science, Institute of Oceanology, Chinese Academy of Sciences, Qingdao 266071, China*

[2] *University of Chinese Academy of Sciences, Beijing 100049, China*

[3] *College of Environment and Safety Engineering, Qingdao University of Science and Technology, Qingdao 266042, China*

[4] *Key Laboratory of Ocean Circulation and Waves, Institute of Oceanology, Chinese Academy of Sciences, Qingdao 266071, China*

Received Jan. 28, 2014; accepted in principle Apr. 4, 2014; accepted for publication Apr. 15, 2014

Abstract To solve nutrient flux and budget among waters with distinct salinity difference for water-salt-nutrient budget, a traditional method is to build a stoichiometrically linked steady state model. However, the traditional way cannot cope appropriately with those without distinct salinity difference that parallel to coastline or in a complex current system, as the results would be highly affected by box division in time and space, such as the Changjiang (Yangtze) River estuary (CRE) and adjacent waters (30.75°–31.75°N, 122°10′–123°20′E). Therefore, we developed a hydrodynamic box model based on the traditional way and the regional oceanic modeling system model (ROMS). Using data from four cruises in 2005, horizontal, vertical and boundary nutrient fluxes were calculated in the hydrodynamic box model, in which flux fields and the major controlling factors were studied. Results show that the nutrient flux varied greatly in season and space. Water flux outweighs the nutrient concentration in horizontal flux, and upwelling flux outweighs upward diffusion flux in vertical direction (upwelling flux and upward diffusion flux regions overlap largely all the year). Vertical flux in spring and summer are much greater than that in autumn and winter. The maximum vertical flux for DIP (dissolved inorganic phosphate) occurs in summer. Additional to the fluxes of the Changjiang River discharge, coastal currents, the Taiwan Warm Current, and the upwelling, nutrient flux inflow from the southern Yellow Sea and outflow southward are found crucial to nutrient budgets of the study area. Horizontal nutrient flux is controlled by physical dilution and confined to coastal waters with a little into the open seas. The study area acts as a conveyer transferring nutrients from the Yellow Sea to the East China Sea in the whole year. In addition, vertical nutrient flux in spring and summer is a main source of DIP. Therefore, the hydrodynamic ROMS-based box model is superior to the traditional one in estimating nutrient fluxes in a complicated hydrodynamic current system and provides a modified box model approach to material flux research.

Keyword: nutrient; box model; hydrodynamic; Changjiang (Yangtze) River estuary

1 INTRODUCTION

Material flux is the important theme of two core projects of the International Global Biosphere Program (IGBP): the Joint Global Ocean Flux Study (JGOFS) and the Land-Ocean Interactions in the Coastal Zone (LOICZ) (Shen, 2001). Estuaries act as important filters and transformers of inorganic and organic materials from river (Li et al., 2011). The degree to which estuaries modify nutrient flux from land to ocean is an important factor affecting the sustainability of near-shore ecosystems and, perhaps over long periods of time, the ocean itself (Nixon et al., 1986).

* Supported by the National Nature Science Foundation of China (Nos. 41121064, 41276116) and the National Basic Research Program of China (973 Program) (No. 2010CB428706)
** Corresponding author: zyu@qdio.ac.cn

Constructing nutrient budgets is an essential tool to examine the relative importance of external nutrient inputs versus physical transports and internal biogeochemical processes (Liu et al., 2009), and to assess nutrient retention including denitrification (Chen and Wang, 1999; Webster et al., 2000). Many studies on nutrient flux have been done using box model (Roson et al., 1997; Simpson and Rippeth, 1998; Ganachaud and Wunsch, 2002; Camacho-Ibar et al., 2003; Proctor et al., 2003; Fang et al., 2007; Hagy and Murrell, 2007; Zhang et al., 2007a; Paetsch and Kuehn, 2008; Kuhn et al., 2010; Padedda et al., 2010).

The Changjiang (Yangtze) River, 6 300 km long, is the longest river in China and the third longest one in the world. Its drainage basin covers an area of about 1.8 million km^2. A huge annual runoff discharge about 29 300 m^3/s enters the Changjiang River estuary (CRE) and adjacent waters. CRE (Fig.1) is a mesotidal, partially-mixed delta estuary with multi-order bifurcations (Li et al., 2011). The hydrographic structure is very complex. Additional to the Changjiang River Discharge (CRD), the Taiwan Warm Current, and Zhejiang Coastal Current flow northwestward from the south and the Yellow Sea Coastal Current southeastward from the north (Tian et al., 1993).

Previously, many studies have been done on nutrient budget and flux in CRE (Liu and Shen, 2001; Huang et al., 2006; Li et al., 2007; Wang and Wang, 2007; Gao et al., 2008; Liu et al., 2009; Chen et al., 2010; Li et al., 2011). In addition, many of them have been finished between the East China Sea and the Kuroshio (Chen et al., 1995; Chen, 1996, 1998; Chen and Wang, 1999; Liu et al., 2000; Wong et al., 2000a, b; Guo et al., 2006; Zhao and Guo, 2011; Guo et al., 2012). Liu and Shen (2001) estimated nutrient flux from the Changjiang River into CRE using a long-term record of nutrient concentration and runoff discharge at Datong Station. Wang and Wang (2007) found nutrient flux upward into the euphotic zone through coastal upwelling were quite large for phosphate. Gao et al. (2008) calculated tidal-averaged budget using physical and chemical hydrography data and suggested that the study area acted as a nutrient sink. Liu et al. (2009) demonstrated that regenerated nutrients in water column and sediment and nutrient flux between the China seas and the open ocean were important for phytoplankton growth. Chen et al. (2010) calculated both input flux from river to estuary and output flux from estuary to coastal zone for phosphate, silicate and nitrate and found that the phosphate and nitrate fluxes were enhanced through estuarine process while silicate flux was unaltered. Li et al. (2011) found that a large amount of input nitrogen was taken up by algae and recycled through denitrification in bottom water and sediment. Therefore, there are great differences in nutrient flux in CRE, the results could not be checked in different box divisions of time and space, and the mechanism could not be deciphered in those studies as hydrodynamic factors were ignored largely. Although Gao et al. (2008) adopted flow velocities into calculation, the results were limited by without enough field data.

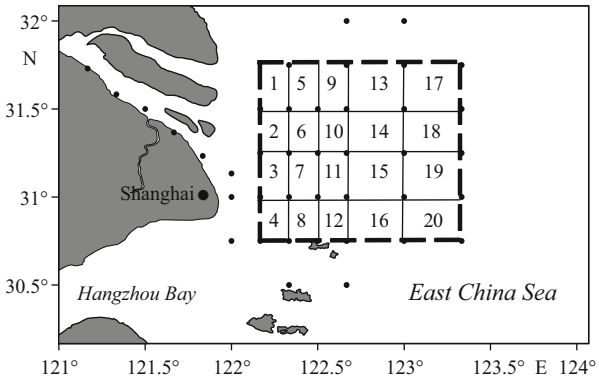

Fig.1 The horizontal box structure, box numbers and boundaries

The LOICZ guidelines for constructing such budgets concentrate on the simplest case where an estuary or embayment is treated as a single box which is well-mixed vertically and horizontally at steady-state (Gordon et al., 1996; Kondratyev and Pozdnyakov, 1996). Further description and application of the LOICZ approach can be found at http://nest.su.se. However, these assumptions can lead to significant and sometimes very large errors depending on the estuary's mixing and geometrical characteristic as well as on the location of the nutrient source (Webster et al., 2000).

First, according to flux concept (certain physical quantity through a given area (usually per unit area perpendicular to flow direction) per unit time), water flux is proportional to velocity and cross-section area (Shen, 2001). Additional to salinity difference, there are temperature and density differences, too. It is defective to estimate water flux according to salinity balance only. Second, only nutrient flux between waters with distinct salinity difference (longitudinal direction or vertical direction with a large depth) can be evaluated in traditional box model, while fluxes parallel to the coastline (transverse) cannot be

evaluated. Third, results are highly affected by the box division in time and space (Webster et al., 2000). Fourth, it is impossible to analyze physical impacts on nutrient flux such as winds, topography, currents, and so the processes and mechanisms cannot be further revealed, either. Fifth, the hydrodynamic characteristics of CRE are complex including penetration, exchange and gradual denaturation (Lie et al., 2003; Chen et al., 2008; Shi and Lu, 2011). Furthermore, main currents in CRE (Subei Coastal Current, Zhejiang Coastal Current, TWC and the branches of CRD beyond the river mouth) are all parallel to the coastline approximately and the salinity of these currents is similar. As CRD fluxes from the west, Subei Coastal Current from the north, Zhejiang Coastal Current and TWC from the south, each has its unique effect on nutrient flux in the study area. It would be erroneous to calculate nutrient flux ignoring hydrodynamic effects (Lie et al., 2003; Shi and Lu, 2011). Water exchange in CRE is too complex to be described by combining water and salt budgets. More analysis on such a complex circulation is required. It may be feasible to develop numerical models of water circulation (Gordon et al., 1996), and imperative to construct a hydrodynamic box model to calculate nutrient flux/transport and to reveal the main processes and mechanisms (Guo et al., 2006).

2 MATERIAL AND METHOD

2.1 Field data

Analysis was based on the data from four cruises in February, May, August and November 2005 in CRE and the adjacent East China Sea, where 40 sampling stations were deployed (Fig.1). Water samples were collected at standard depths, i.e., 0, 5, 10, 20, 30 m from surface and 2 m above bottom. Nitrate (NO_3-N), ammonium (NH_4-N), nitrite (NO_2-N), dissolved inorganic phosphorus (DIP) and suspended particulate matter (SPM) were measured for concentration. An aliquot of water was filtered onboard through pre-combusted Whatman GF/F filters. 0.2% chloroform was added to the filtrate. All samples were preserved in polyethylene bottles (pre-conditioned for 24 h in 1:10 hydrochloric acid solution) and deep frozen in dark. NO_3-N was measured using the cadmium-zinc reduction method, NH4-N using the indophenol blue method (Grasshoff et al., 2009), NO_2-N using the Griess-Ilosvay method (Barnes, 1959) and PO_4-P using the phosphomolybdenum blue method (Strickland and Parsons, 1968; Pai et al., 1990). Data quality was monitored using inter-calibrations and precision was estimated using repeated determinations of selected samples. The concentration of dissolved inorganic nitrogen (DIN) was calculated as the sum of NO_3-N, NO_2-N, and NH_4-N. Samples of SPM were dried at 60°C before weighing (Li et al., 2011).

2.2 Model configuration

We employ the box model by Officer (1980) with some modifications. This method is basically the same as that used by the ERSEM (European Regional Seas Ecosystem Model) developed for the North Sea (Baretta et al., 1995; Blackford and Radford, 1995; Lenhart et al., 1995; Moll and Radach, 2003; Radach and Moll, 2006; Schrum et al., 2006a, b). We used the Regional Ocean Model System (ROMS) (Shchepetkin and McWilliams, 2005) as our hydrodynamic model that has been successfully implemented in the East China Sea and verified against field data and previous studies (Mao et al., 1963; Lie et al., 2003; Lee et al., 2004; Chen et al., 2008; Isobe, 2008; Liu et al., 2008a, b; Gao et al., 2009; Shi and Lu, 2011). Since the hydrodynamics in the study area are very complicated (as tides mixing with the interaction of different water types) (Zhang et al., 2007b), ocean dynamics in a big domain (99°–150°E, 0°–50°N) was first simulated. The horizontal resolution was 1/12°×1/12° and there were 24 s-levels in the vertical. The bottom topography was derived from the Etopo2 (version 2) dataset while the air-sea flux, wind stress, SST, and SSS data were from COADS05. The data of CRD was 35-year mean monthly data of the Datong hydrological station. The initial and open boundary conditions were from SODA (Simple Ocean Data Assimilation) products. Four main tidal constituents (M2, S2, K1, and O1) were imposed at the open boundaries. The Mellor and Yamada level 2.5 turbulence closure scheme was utilized. The model was spun up for 10 years to reach its equilibrium, and then the modeled outputs (temperature, salinity, SSH and fluid fields) were served as the initial and boundary conditions for a smaller domain (119°–126.8°E, 27.5°–35.8°N). The small domain had the same 24 vertical layers as in the big domain while the horizontal resolution was enhanced (1/24°×1/24°). After running the model for 10 years, model outputs for 2005 were adapted to the boxes (30.75°–31.75°N, 122°10′–123°20′E).

The concept, structure and implementation of ERSEM are omitted for brevity. The boxes were defined according to morphological, hydrographic and biological properties, and the field data (Fig.1).

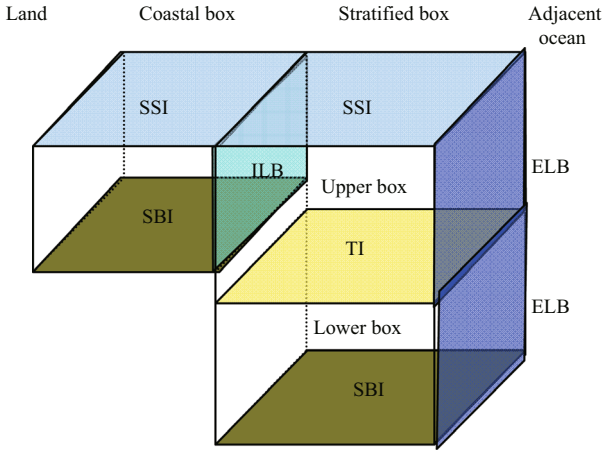

Fig.2 The internal box structure of the CRE

TI: thermocline interface; ILB: interior lateral boundary; ELB: exterior lateral boundary; SBI: sea bed interface; SSI: sea surface interface.

Each dot represented a survey station. Twenty boxes (denoted 1 to 20) were defined. Four dotted lines represented boundaries in the north, south, east and west, respectively.

The thermocline interface was set at 20 m between the upper and lower layers according to the field data (Fig.2). The flow across the boundaries of the boxes was calculated from the velocity components given on the grid from ROMS model: The east-west boundaries of the boxes were aligned to pass the v-points and the north-south boundaries of the boxes were aligned to pass the u-points of the grid. The horizontal boundaries of the boxes were aligned to pass the w-points of the grid. The velocity components were integrated over each interface to give the flow perpendicular to the interface.

The transports were divided into the horizontal and vertical parts. The horizontal transports were restricted to the horizontal advection parts of the flow neglecting the dispersion several orders of magnitude less than the advection, while the vertical transports consist of a diffusion and an advection parts of the flow. The equation is written as:

$$\frac{\mathrm{d}C}{\mathrm{d}t} = C_{\mathrm{hai}} - C_{\mathrm{hao}} + C_{\mathrm{vai}} - C_{\mathrm{vao}} + C_{\mathrm{vdi}} - C_{\mathrm{vdo}} + C_{\mathrm{ri}} + C_{\mathrm{cb}}, \quad (1)$$

in which: $C_{\mathrm{hai}}/C_{\mathrm{hao}}$: horizontal advection transport (inflow/outflow); $C_{\mathrm{vai}}/C_{\mathrm{vao}}$: vertical advection transport between upper and lower boxes (inflow/outflow); $C_{\mathrm{vdi}}/C_{\mathrm{vdo}}$: vertical diffusion transport between upper and lower boxes (inflow/outflow); C_{ri}: riverine input; C_{cb}: chemical and biological reactions.

$$C_{\mathrm{hai}} = \sum_{j=1}^{n} A_i F_{\mathrm{in}i} C_i, \quad (2)$$

where n: the number of lateral boundaryies; A_i: the area of lateral boundary of the adjacent box i (i=1 to n); $F_{\mathrm{in}i}$: flow into a box through the area A_i, given by ROMS simulation integrated for 30 day; C_i: concentration outside of adjacent box i to area A_i from field data.

$$C_{\mathrm{hao}} = \sum_{i=1}^{n} F_{\mathrm{ou}i} A_i C, \quad (3)$$

where $F_{\mathrm{ou}i}$: flow out of the box through the area A_i, given by ROMS simulation integrated for 30 day; C: nutrient concentration in the box from field data.

In the case of upward transport:

$$(C_{\mathrm{vai}})_{\mathrm{U}}=Q_{\mathrm{v}}C_{\mathrm{L}},\ (C_{\mathrm{vai}})_{\mathrm{L}}=0,$$
$$(C_{\mathrm{vao}})_{\mathrm{L}}=Q_{\mathrm{v}}C_{\mathrm{L}},\ (C_{\mathrm{vao}})_{\mathrm{U}}=0, \quad (4)$$

In the case of downward transport:

$$(C_{\mathrm{vai}})_{\mathrm{U}}=0,\ (C_{\mathrm{vai}})_{\mathrm{L}}=Q_{\mathrm{v}}C_{\mathrm{U}},$$
$$(C_{\mathrm{vao}})_{\mathrm{L}}=0,\ (C_{\mathrm{vao}})_{\mathrm{U}}=Q_{\mathrm{v}}C_{\mathrm{U}}, \quad (5)$$

where Q_{v}: vertical flux through the area between the upper and the lower box given by ROMS simulation integrated for 30 day; C_{U}: concentration in the upper box; C_{L}: concentration in the lower box from field data; The subscripts U and L denote the upper and the lower box, respectively.

If $C_{\mathrm{L}}>C_{\mathrm{U}}$,

$$(C_{\mathrm{vdi}})_{\mathrm{U}} = D_{\mathrm{v}} \cdot A \cdot (C_{\mathrm{L}} - C_{\mathrm{U}}) / L,\ (C_{\mathrm{vdi}})_{L} = 0,$$
$$(C_{\mathrm{vdo}})_{\mathrm{L}} = D_{\mathrm{v}} \cdot A \cdot (C_{\mathrm{L}} - C_{\mathrm{U}}) / L,\ \ (C_{\mathrm{vdo}})_{\mathrm{U}} = 0, \quad (6)$$

If $C_{\mathrm{L}}<C_{\mathrm{U}}$,

$$(C_{\mathrm{vdi}})_{\mathrm{L}} = D_{\mathrm{v}} \cdot A \cdot (C_{\mathrm{U}} - C_{\mathrm{L}}) / L,\ (C_{\mathrm{vdi}})_{\mathrm{U}} = 0,$$
$$(C_{\mathrm{vdo}})_{\mathrm{U}} = D_{\mathrm{v}} \cdot A \cdot (C_{\mathrm{U}} - C_{\mathrm{L}}) / L,\ (C_{\mathrm{vdo}})_{\mathrm{L}} = 0, \quad (7)$$

where D_{v}: the local vertical diffusion coefficients (0.0001 was adopted) (Zhang and Zhao, 2007; Zhu et al., 2008, 2009); L: the length scale of vertical diffusion (20 m according to references (Eigenheer et al., 1996; Gao et al., 2009)); A: the area of interface between the upper and lower boxes.

2.3 Adaptation of flow fields to boxes (in Matlab)

In the case of east-west lateral boundary,

$$F_j = \sum_{k=1}^{n} \Delta x_k \cdot D_k.$$

In the case of north-south lateral boundary,

$$F_j = \sum_{k=1}^{n} \Delta y_k \cdot D_k, \quad (8)$$

n: number of grids in the east-west or north-south side of lateral boundary to the adjacent box j; k: serial number of grids in the east-west or north-south side of lateral boundary to the adjacent box j; $\Delta x/\Delta y$: side length of the settled in ROMS model; D_k: the depth of gird k in the east-west or north-south side of lateral boundary to the adjacent box j.

$$U_j^i = (1/M) \cdot \sum_{K=1}^{M} v_K \,, \tag{9}$$

M: total number of grids in the lateral boundary to the adjacent box j; K: serial number of grids in the lateral boundary to the adjacent box j; v_K: flow of gird K into the box through the area F_j, given by ROMS simulation integrated for 30 day.

The equation for U_j^o, can be inferred to U_j^i and omitted for brevity.

2.4 Flow adjustment for fixed box volumes

Due to the restriction of the fixed box volumes, the effects of the varying sea surface elevation could not be taken into account. Since a mass balance equal to zero has to be achieved, the seasonal transport values were corrected by a non-linear optimization method in Matlab (Ma, 2010).

3 RESULT

3.1 Horizontal nutrient fluxes

Horizontal nutrient fluxes for DIN (dissolved inorganic nitrate), DSI (dissolved inorganic silicate) and DIP (dissolved inorganic phosphate) for four seasons were calculated. 2D flux fields were in Figs.3 & 4. UL, LL in tables and figures stands for upper layer and lower layer, respectively. The maximum and minimum fluxes, and the corresponding locations are in the Appendix A. Results show that the flux value, direction, nutrient structure, and distribution in the horizontal varied significantly over time and space.

In winter in upper layer, both fluxes of DIN (21.49–0.029 mmol/(m^2·s)) and DSI (15.59–0.037 mmol/(m^2·s)) decreased gradually from the shore to the open seas. While DIP flux (0.40–0.002 5 mmol/(m^2·s)) decreased first and then increased at around 122.75°E, which agrees with Zhang et al (2007a)'s findings and will be explained in Section 4.1. Fluxes flowed southward overall, but turned southeastward in the expansion area of the Changjiang Diluted Water (CDW). Of particular interest was the narrow band alongshore for major DIN flux (≥50% of the maximum flux), while major DIP flux was distributed more evenly over the study area. For major DSI flux, it was distributed more evenly than major DIP flux but less evenly than major DIN flux. In lower layer, fluxes of DIN (0.40–0.000 81 mmol/(m^2·s)), DSI (0.71–0.001 2 mmol/(m^2·s)) and DIP (0.033–0.000 072 mmol/(m^2·s)) were all greater in the northern region (30.75°–32°N) than in the middle (31.25°–30.75°N) and southern regions (30.75°–30.5°N). They flowed southward overall and turned southeastward in the middle region (30.75°–31.25°N).

In spring in upper layer, the maximum flux was found around the CRE mouth. Major fluxes of DIN (2.95–0.030 mmol/(m^2·s)), DSI (4.86–0.092 mmol/(m^2·s)) and DIP (0.048–0.000 71 mmol/(m^2·s)) were all made up of two parts. One was a narrow band west of 122.25°E, the other was around TWC-influenced area (122.25°–123°E, 30.5°–31.5°N), extending northeastward like an arc to the high-frequency occurrence area of harmful algae bloom (HAB). Fluxes flowed northward approximately displaying two notable features. One was the high flux patch near the CRE mouth. The other was the greater impact from the open seas fluxes on DIP flux than on DIN or DSI fluxes. The magnitude of the patch was several folds higher than that of ambient waters, and its direction turned northeastward with CDW. In lower layer, fluxes of DIN (0.51–0.002 6 mmol/(m^2·s)), DSI (1.28–0.011 mmol/(m^2·s)) and DIP (0.024–0.000 16 mmol/(m^2·s)) were all distributed evenly over the whole region, flowing northward in the south of 31.25°N and turning northwestward north of 31.25°N.

In summer in upper layer, a narrow band west of 122.25°E occurred for major fluxes of DIN (7.92–0.019 mmol/(m^2·s)), DSI (10.67–0.022 mmol/(m^2·s)) and DIP (0.15–0.000 38 mmol/(m^2·s)). Fluxes in the band south of 31.5°N were greater than those north of 31.5°N, flowing northward overall. In lower layer, fluxes of DIN (1.05–0 mmol/(m^2·s)), DSI (2.26–0 mmol/(m^2·s)) and DIP (0.04–0 mmol/(m^2·s)) were similar to those in spring in distribution and direction, except for the difference north of 31.25°N where fluxes turned less westward.

In autumn in upper winter, fluxes of DIN (7.45–0.13 mmol/(m^2·s)), DSI (10.23–0.2 mmol/(m^2·s)) and DIP (0.13–0.006 3 mmol/(m^2·s)) were similar to those in winter, decreasing gradually from the shore to the open seas, but more evenly distributed. Fluxes flowed southward largely. In lower layer, fluxes of DIN (0.29–0.009 9 mmol/(m^2·s)), DSI (0.46–0.019 mmol/(m^2·s))

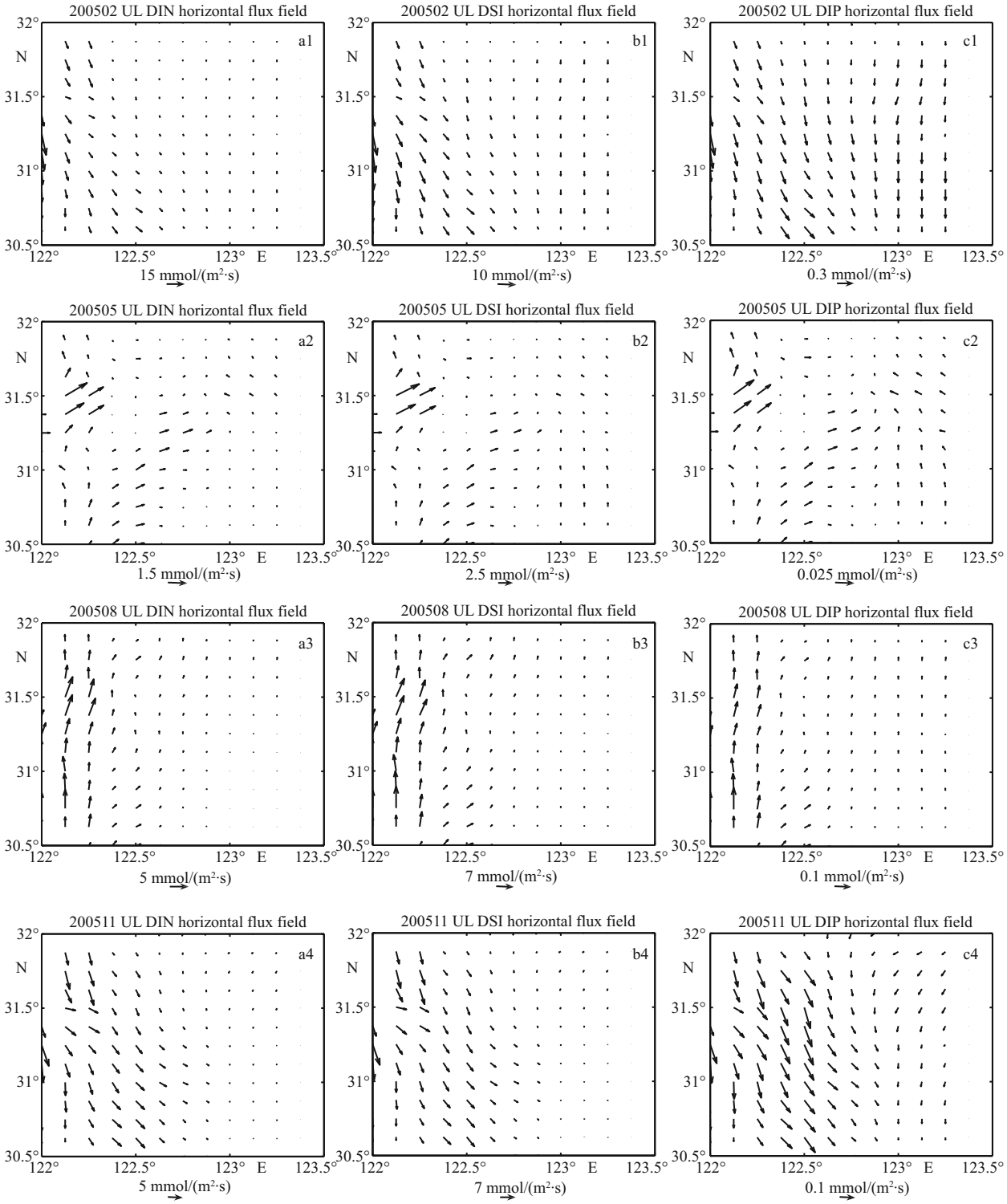

Fig.3 Horizontal fluxes in upper layer for four seasons

and DIP (0.011–0.000 52 mmol/(m²·s)) were all greater in the southern and northern regions (30.5°–30.75°N, 31.25°–32°N) than in the middle region (30.75°–31.25°N), flowing northwestward north of 30.75°N and southwestward south of 30.75°N.

Structure of nutrient flux is shown in Figs.5 & 6 and the Appendix A. All the ratios of DIN/DIP, DSI/DIP and DIN/DSI decreased from the shore to the open seas, with isolines in parallel to the coastline approximately. An exception is that DIN/DSI

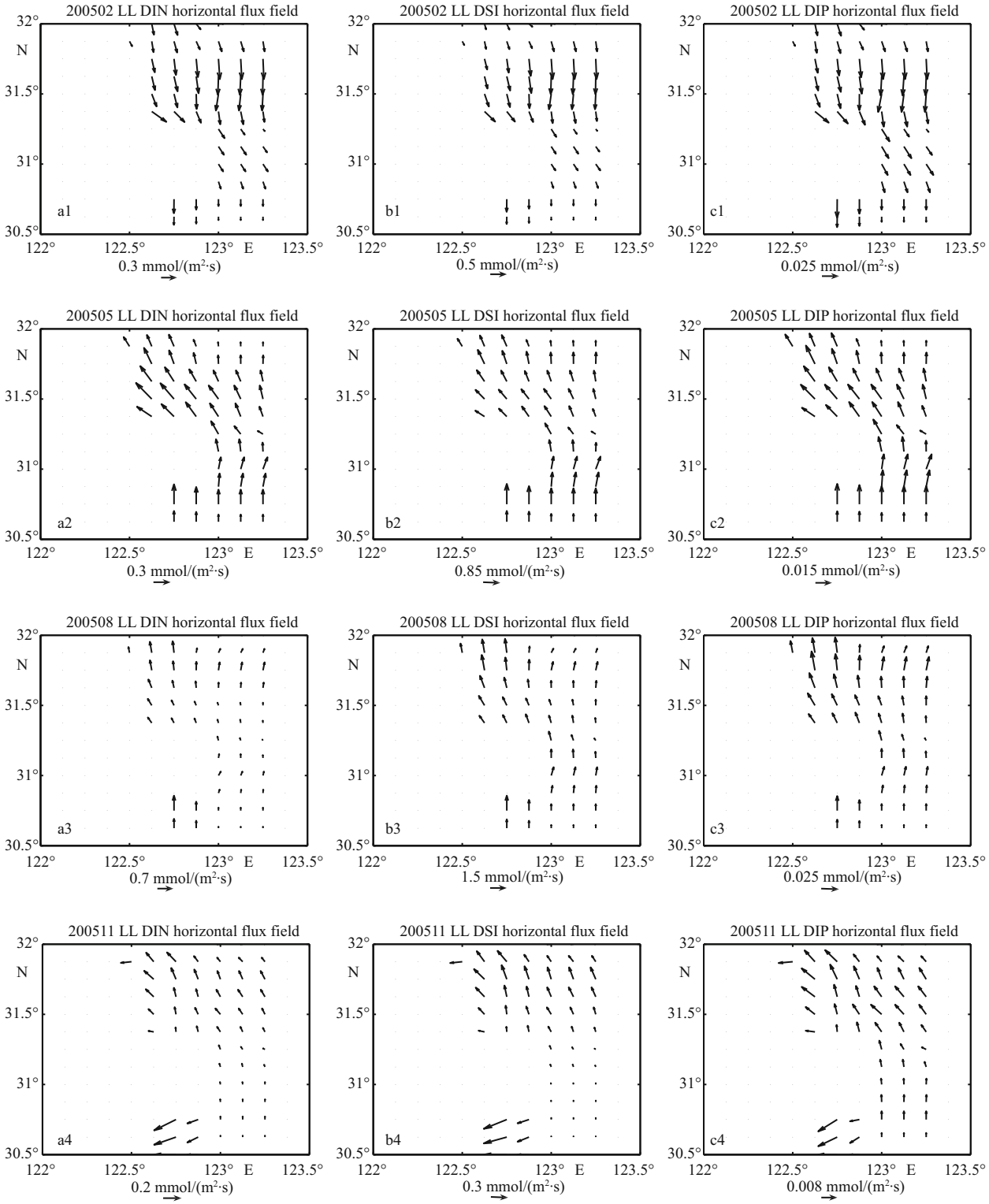

Fig.4 Horizontal fluxes in lower layer for four seasons

increased seaward in autumn, which is discussed in Section 4.1. The structure in upper layer varied in a wider range than in lower layer. Nutrient fluxes from the lower layer and the open seas could bring down the ratios of DIN/DIP and DSI/DIP.

3.2 Vertical nutrient fluxes

Vertical nutrient fluxes (advection and diffusion fluxes) were opposite in size in the upper and lower layers. For brevity, only vertical nutrient fluxes in

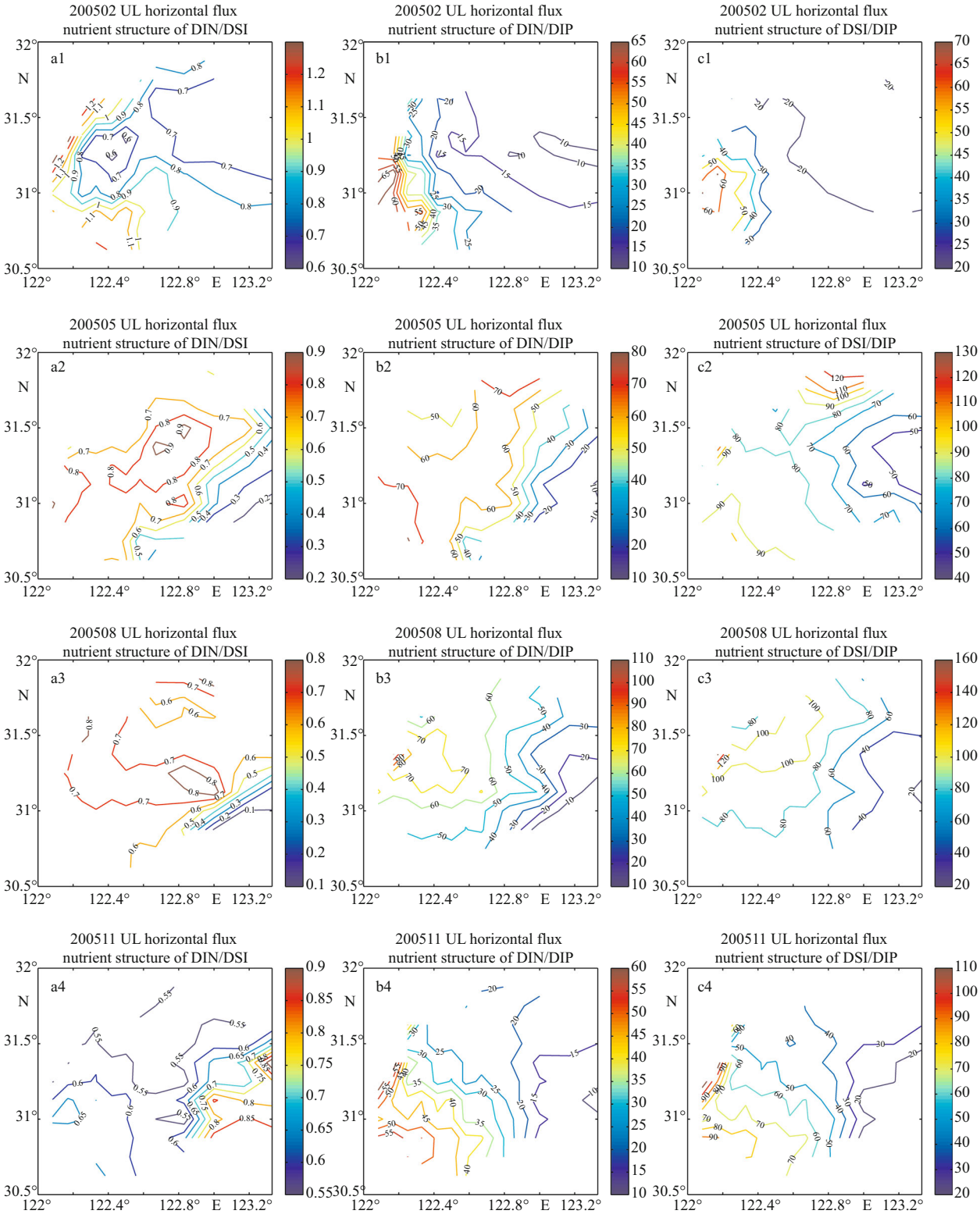

Fig.5 Structure of horizontal nutrient flux in upper layer for four seasons

upper layer are described in Table 1, Figs.7 & 8, and the Appendix B. Vertical nutrient fluxes refers to upwelling and upward diffusion fluxes next, with downward fluxes omitted. The value, area and structure of vertical nutrient fluxes varied significantly in season. The overall picture of upwelling we obtained is consistent with previous studies (Lü et al., 2006, 2007; Pei et al., 2009).

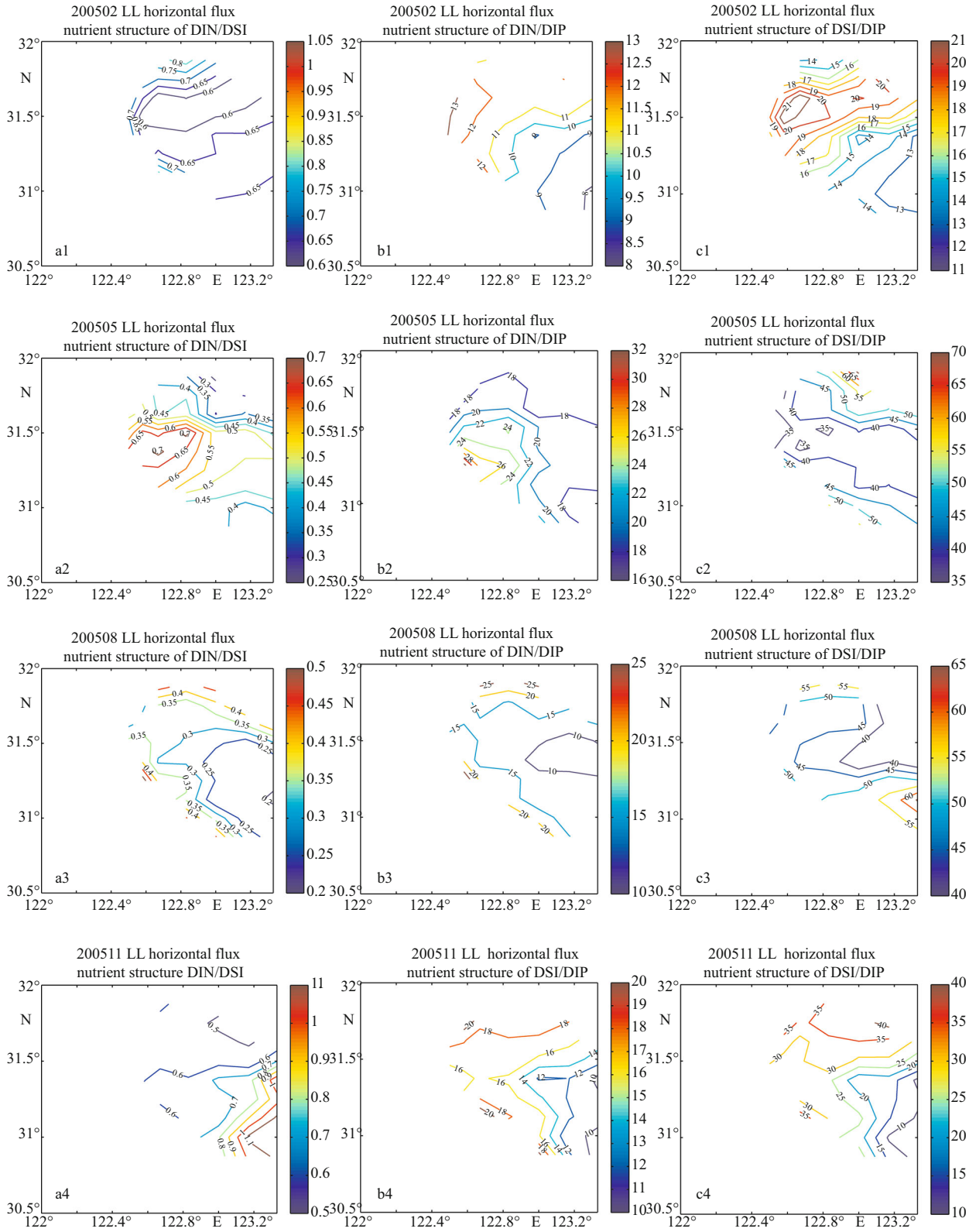

Fig.6 Structure of horizontal nutrient flux in lower layer for four seasons

DIN, DSI, and DIP fluxes in winter upwelling (122.48, 193.35, and 12.39 mol/s in 9 139 km^2), and those in upward diffusion (8.4 mol/s in 2 788 km^2, 35.52 mol/s in 5 576 km^2, and 1.20 mol/s in 23 063 km^2, respectively) were all in the northeast region. Fluxes in spring upwelling (6 507 km^2) (DIN

Table 1 Location, area, and nutrient structure of vertical nutrient fluxes

Item	Longitude (°E)	Latitude (°N)	Area (km^2)	Ratios of DIN/DSI/DIP
		200502		
Upwelling	East of 122.75°E	31°–32°N	9 139	10:16:1
Upward diffusion	Near 123°E (east of 122.5°E for DSI, near 122.5°E for DIP)	31.5°–32°N (31.25°–32°N for DSI)	2 788 (5 576 for DSI, 23 063 for DIP)	7:30:1
		200505		
Upwelling	Near 123°E	30.75°–31.5°N	6 507	23:46:1
Upward diffusion	East of 123°E	30.75°–31.5°N (30.5°–31.5°N for DIP)	2 788 (10 533 for DIP)	12:6:1
		200508		
Upwelling	Near 123°E	30.75°–31.5°N	4 975	19:48:1
Upward diffusion	East of 123°E (east of 122.5°E for DIP)	30.75°–31.5°N (30.75°–31.75°N for DIP)	2 788 (4182 for DSI, 12 702 for DIP)	5:28:1
		200511		
	Near 122.5°E	31.5°–32°N		
Upwelling	Near 123°E	30.75°N	5 888	18:27:1
	East of 123°E	31.5°N		
	East of 123°E for DSI	31.5°N for DSI		
Upward diffusion	Around 123°E	31.5°–32°N	1 394 for DSI, 8 364 for DIP	0:1.8:1
	East of 123°E for DIP	30.75°–31.75°N for DIP		

131.45 mol/s, DSI 262.45 mol/s, and DIP 5.65 mol/s) and in summer upwelling (4 975 km^2) (108.81, 282.64, and 5.83 mol/s, respectively) were all in the eastern region (between 31°N and 31.625°N) mostly. Spring upward diffusion fluxes (DIN 37.02 mol/s in 2 788 km^2, DSI 19.15 mol/s in 2 788 km^2, and DIP 3.20 mol/s in 10 533 km^2) and summer upward diffusion fluxes (DIN 25.68 mol/s in 2 788 km^2, DSI 152.75 mol/s in 4 182 km^2, and DIP 5.55 mol/s in 12 702 km^2) were confined in the eastern region (between 31°N and 31.75°N). For autumn upwelling (5 888 km^2), fluxes (DIN 87.06 mol/s, DSI 134.29 mol/s, and DIP 4.96 mol/s) were scattered mainly in the northeast, southeast and northwest regions; and for upward diffusion, fluxes (DIN 0, DSI 1.63 mol/s in 1 394 km^2 and DIP 0.92 mol/s in 8 364 km^2) were mainly in the northeast, southeast regions.

There was a large overlap of upwelling and upward diffusion regions in the same season. The area of DIP flux was the biggest, followed by DSI and DIN fluxes in turn. The maximum DIP flux from upwelling (5.83 mol/s) and upward diffusion (5.55 mol/s) were both in summer. Next, we compare nutrient fluxes in vertical and horizontal directions. Vertical nutrient flux showed higher DIP, DSI and lower DIN. E.g., in spring, horizontal fluxes were 3 to 7 times (DIN) and 3 to 5 times (DSI) greater than vertical ones. While for DIP they were about comparable. In summer, horizontal fluxes were 3 to 6 times (DIN), 5 to 10 times (DSI) and 5 to 8 times (DIP) greater than vertical counterparts. In autumn and winter, vertical fluxes were 2 orders of magnitude below the horizontal. Although in summer vertical flux for DIP was the maximum, the horizontal one was even greater. Therefore, the vertical DIP flux was the greatest in spring, followed by summer, while in autumn and winter, negligible. Spring vertical DIP flux was an important source.

3.3 Boundary nutrient fluxes

Four boundaries are plotted in Fig.1. Cross-boundary nutrient fluxes are the sum of those in all layers. The western boundary fluxes represent fluxes to/from coastal currents affected by the Changjiang River mainly; the eastern boundary fluxes represent fluxes to/from the eastern open seas; the northern boundary fluxes represent fluxes to/from the northern open seas affected by Subei Coastal current and the south Yellow Sea currents mainly; the southern boundary fluxes represent fluxes to/from the southern open seas affected by TWC and Zhejiang Coastal Current mainly. Unit of mol/s was adopted to examine nutrient exchange and transport between the study

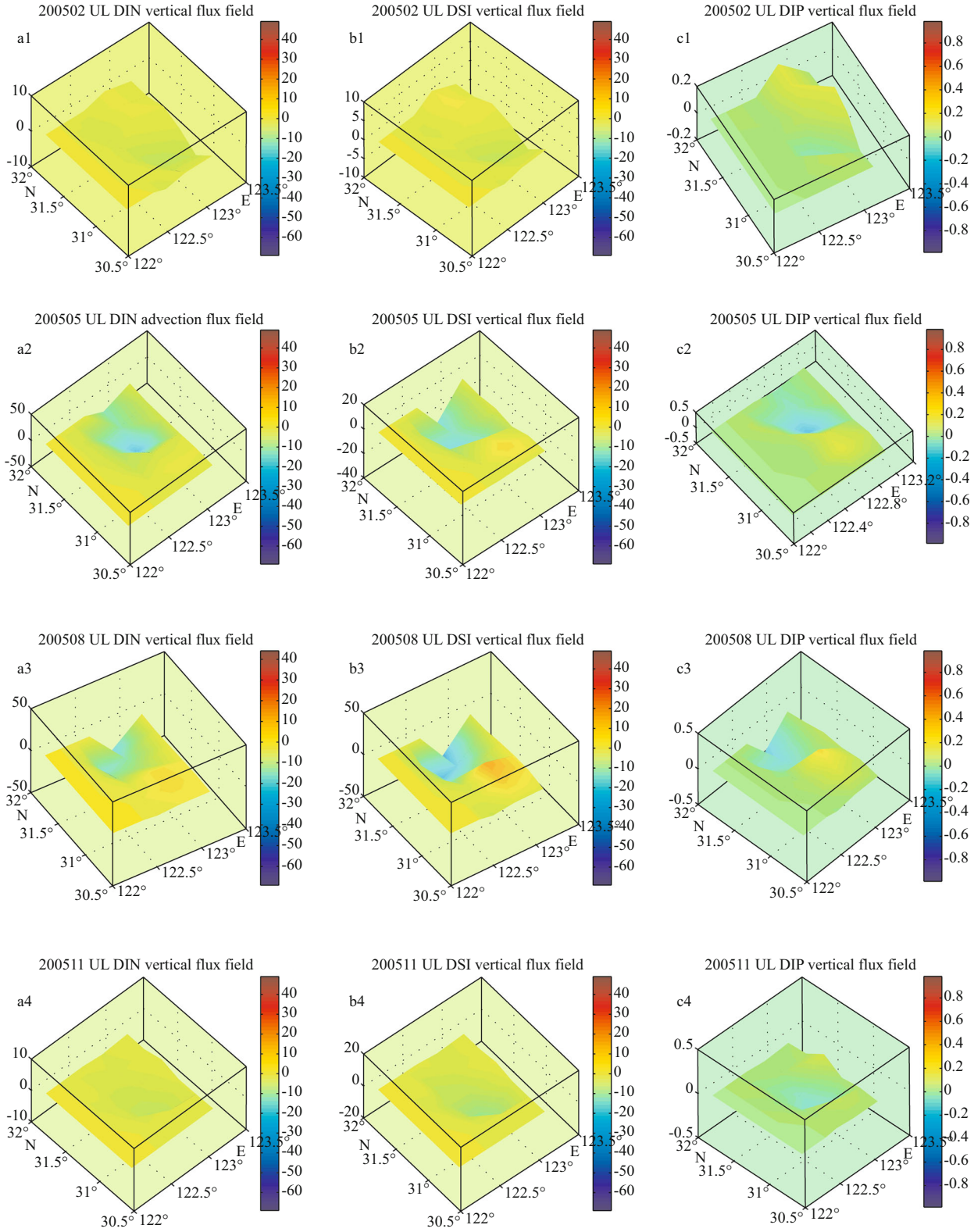

Fig.7 Vertical fluxes (advection and diffusion) in upper layer for four seasons

*z*label: 10^{-5} mmol/(m^2·s).

area and exterior waters. The boundary nutrient flux value, direction and nutrient structure varied significantly in season (Table 2 and the Appendix A).

In winter, at eastern boundary, fluxes in the upper and lower layers were opposite in size nearly. The outflow fluxes across the southern boundary almost doubled the

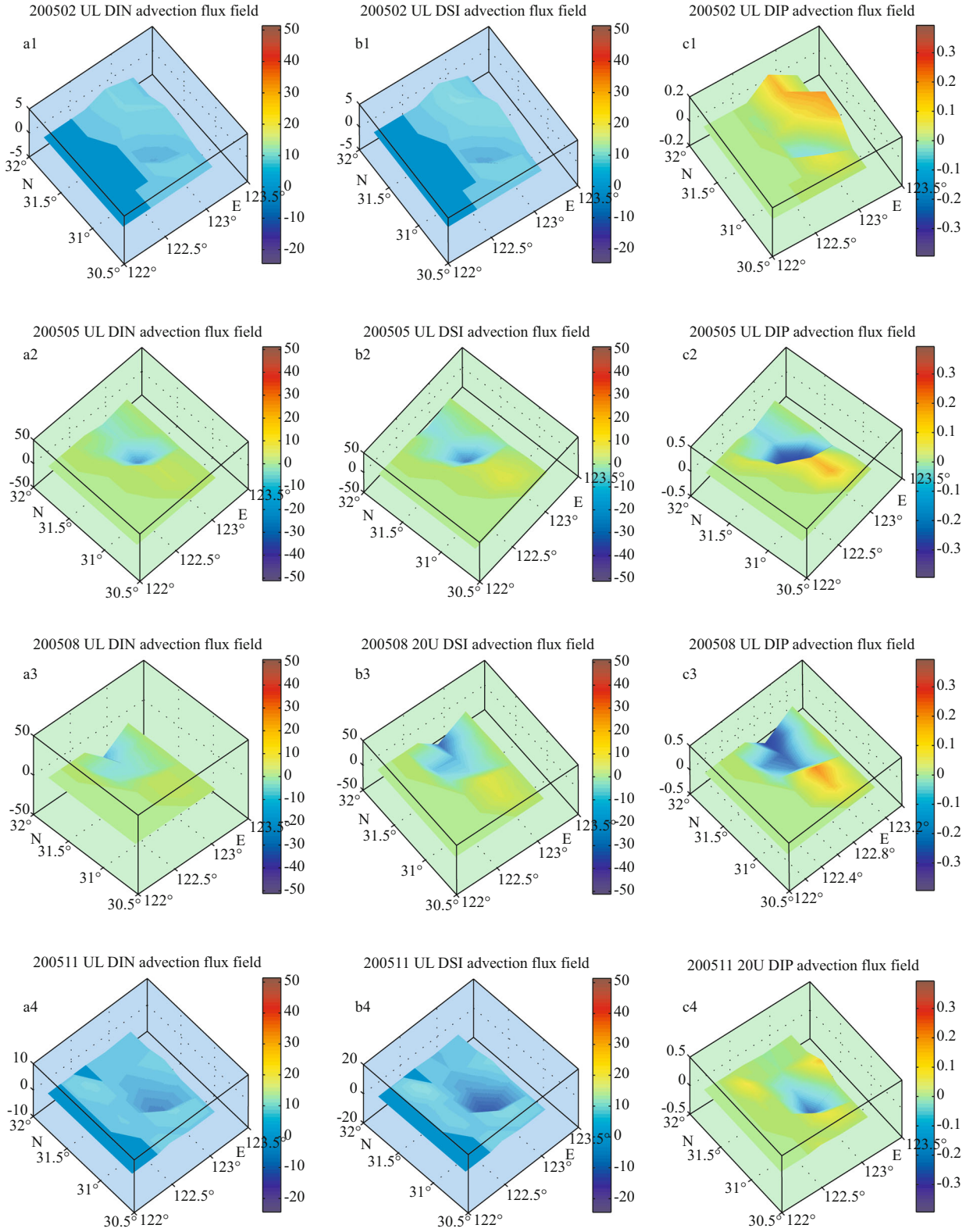

Fig.8 Vertical advection fluxes in upper layer for four seasons

*z*label: 10^{-5} mmol/(m^2·s).

inflow across the northern boundary, exceeding total inflow of northern and western boundary fluxes.

In spring, at southern and northern boundaries, flux in upper layer was greater than that in lower layer for DIN, while it was opposite for DSI and DIP whose fluxes in lower layer were greater, for example, DIP

Table 2 Boundary nutrient fluxes

Item		Eastern boundary (mol/s	mmol/(m²·s))	Western boundary (mol/s	mmol/(m²·s))	Southern boundary (mol/s	mmol/(m²·s))	Northern boundary (mol/s	mmol/(m²·s))
DIN	UL	18.16	0.04	4 781.05	4.22	-15 011.83	-4.90	7 486.39	2.73
DIN	LL	-15.73	-0.02	0.00	0.00	-276.08	-0.18	533.19	0.35
DSI	UL	27.25	0.05	3 976.06	3.51	-15 470.22	-5.04	8 135.12	2.97
DSI	LL	-26.01	-0.04	0.00	0.00	-449.37	-0.29	880.65	0.58
DIP	UL	1.82	0.00	82.21	0.07	-507.55	-0.17	357.81	0.13
DIP	LL	-1.95	0.00	0.00	0.00	-32.88	-0.02	44.90	0.03
					200505				
DIN	UL	46.03	0.09	871.01	0.77	653.77	0.21	-733.52	-0.27
DIN	LL	0.08	0.00	0.00	0.00	635.22	0.40	437.21	-0.29
DSI	UL	172.59	0.35	1 480.63	1.31	1 396.89	0.46	-1 122.49	-0.41
DSI	LL	-13.02	-0.02	0.00	0.00	1 698.54	1.08	-1 196.64	-0.79
DIP	UL	3.67	0.01	12.59	0.01	15.09	0.00	-15.09	-0.01
DIP	LL	-0.09	0.00	0.00	0.00	34.88	0.02	-25.08	-0.02
					200508				
DIN	UL	-23.36	-0.05	1 038.28	0.92	5 488.00	1.79	-4 331.66	-1.58
DIN	LL	-11.77	-0.02	0.00	0.00	516.50	0.33	-691.08	-0.45
DSI	UL	-28.97	-0.06	1 533.57	1.35	9 360.70	3.05	-6 396.77	-2.33
DSI	LL	-29.45	-0.05	0.00	0.00	1 543.67	0.98	-1 866.41	-1.22
DIP	UL	-0.50	0.00	10.44	0.01	137.63	0.04	-92.27	-0.03
DIP	LL	-0.90	0.00	0.00	0.00	27.22	0.02	-45.93	-0.03
					200511				
DIN	UL	84.53	0.17	2 256.56	1.99	-5 389.97	-1.76	4 610.42	1.68
DIN	LL	14.32	0.02	0.00	0.00	-16.74	-0.01	-185.22	-0.12
DSI	UL	123.06	0.25	3 912.29	3.45	-8 679.90	-2.83	8 517.17	3.11
DSI	LL	20.00	0.03	0.00	0.00	-47.38	-0.03	-401.48	-0.26
DIP	UL	6.38	0.01	39.16	0.03	-144.04	-0.05	142.42	0.05
DIP	LL	1.21	0.00	0.00	0.00	2.49	0.00	-10.04	-0.01

'-' stands for outflow.

flux in lower layer nearly doubled that in upper layer. At eastern boundary, flux in upper layer was greater than that in lower layer. Inflow at southern boundary was slightly greater than outflow at northern boundary. The study area acted as a nutrient sink as a whole, which is supported by the findings by Gao et al. (2008).

In summer, although scenarios are similar to those in spring, some differences do exist. At southern and northern boundaries, flux in upper layer was much greater than that in lower layer. Inflow flux at southern boundary was much greater than outflow at northern boundary. At eastern boundary, flux in upper layer was greater than that in lower layer for DIN, while it was opposite for DSI and DIP, greater in upper layer.

Scenarios in autumn and winter are similar. At southern, western, and northern boundaries, fluxes were all much greater in upper layer than in the lower. In addition, fluxes in the two layers at northern boundary were opposite in direction. The outflow at southern boundary was slightly greater than the inflow at the northern boundary.

4 DISCUSSION

4.1 Characteristics and mechanisms of horizontal nutrient fluxes

In contrast to previous studies which multiplied nutrient concentrations by discharge at Datong Station

(Liu and Shen, 2001; Duan et al., 2008), horizontal nutrient fluxes obtained were under a complex current system forced by a hydrodynamic model considering physical factors. The flux nutrient structure we obtained is similar to that in previous studies (Chai et al., 2006, 2009; Gong et al., 2006, 2007; Wang, 2006; Wang et al., 2008; Gao et al., 2009; Chen et al., 2010; Han et al., 2012), indicating reliability of our result.

Horizontal water flux reflected characteristics of water currents in the study area (Appendix B. 2). The diversion of CDW has been observed distinctly in spring and summer; TWC is stronger in spring than in summer; the magnitude of horizontal water flux in lower layer was 1/10 of that in upper layer in autumn and winter, a half in summer, and similar in spring; consistent with previous studies (Mao et al., 1963; Zhu et al., 2004; Pei et al., 2008; Gao et al., 2009).

We compared the horizontal water flux and horizontal nutrient fluxes. Surprising similarities of spatial difference and seasonal variation were found, suggesting that the horizontal nutrient flux was affected more by physical dilution than by biochemical processes in water column. This has been reported in many previous studies (Tian et al., 1993; Ganachaud and Wunsch, 2002; Chang and Isobe, 2003; Zhu et al., 2006; Yan et al., 2008; Shi and Lu, 2011). On the other hand, an only exception was greater horizontal water flux but smaller horizontal fluxes in upper layer of the open seas than nearshore in summer and spring, which might be caused by the extremely low nutrient concentration there due to high primary production.

In addition, flux in upper layer exceeded that in lower layer by tens of folds and varied in a wider range, which indicates that horizontal nutrient fluxes depend more on flux in upper layer. In upper layer, what made the greatest difference in both horizontal nutrient fluxes and water flux was not in the east-west component, but in the north-south component, suggesting that horizontal nutrient fluxes might be controlled by a north-south factor: the monsoon. This will be verified in future studies.

Horizontal nutrient fluxes depend on the complex current system (Zhang et al., 2007a). The influence of CRD was up to 123°E in autumn and winter, but confined to a bind west of 122.25°E in spring and summer. This suggests TWC might be responsible for the restricting of the influence of CRD in non-monsoon seasons.

Unlike DIN and DSI fluxes decreasing gradually from shore to ocean, DIP flux appears to be more evenly distributed, which could be explained by the effect of the open seas flux to the east , or the comparable vertical DIP flux (discussed in Section 4.2), or phosphate kinetic buffer mechanism (Froelich, 1988). Therefore, the unique characteristics for DIP flux of decreasing first and then increasing from shore to ocean in winter took shape. Moreover, in spring, because of great water flux and high nutrient concentration near the river mouth, the nutrient flux patch formed. Another high nutrient flux region going northeastward along the coast and then turning eastward to the east of Zhoushan Islands, and then to the high-frequency HAB occurrence area was in believe due to nutrient-rich TWC northeastward invasion.

4.2 Characteristics and mechanisms of vertical nutrient fluxes

Upwelling was found to exist all the year round with remarkable seasonal and spatial variation, which was confirmed by cruise observations, satellite sea surface temperature (SST), and SST climatologic data by Lü et al. (2006) and Wang and Wang (2007). However, the areas of upwelling we obtained were different from that by Wang and Wang (2007), probably because of high frequency factors. e.g., winds, crucial to upwelling (Lie et al., 2003). Strong upwelling in spring and summer is due probably to large CRD and TWC intrusion (Lü et al., 2006). In spring and summer, the study area features stronger upwelling and larger difference in concentration between upper and lower layers, resulting in greater vertical nutrient fluxes than those in autumn and winter in general, as reported also by Chen et al. (2004) previously.

Vertical nutrient flux in spring are almost one magnitude smaller than that of Pei et al. (2009), to which we explain as being caused mainly by the different upwelling velocities adopted. Pei et al. (2009) used 1×10^{-5}–5×10^{-5} m/s while only 10^{-6} and even 10^{-7} m/s in magnitude based on the model. In summer, vertical nutrient fluxes are almost identical to those in spring, which is in contrast to the conclusion in Pei et al. (2009) that summer upwelling affects slightly the upper water. The depth for calculation by Pei et al. (2009) is 10 m, while it is 20 m in this study. It is understandable that upwelling would become weaker as depth shallows. With the addition of high frequency factors essential to upwelling such as winds, it is suggested that vertical nutrient flux might be highly variable in time and space. In addition, in autumn and winter, vertical turbulence is strong, the

vertical nutrient fluxes may be overestimated (e.g. upwelling area of 9 139 km^2, upwelling flux of 12.39 mol/s for DIP in winter). In addition, vertical nutrient fluxes in autumn and winter are neglected in previous studies, calling for more studies in the future.

Upwelling fluxes exceeded upward diffusion fluxes all the year round. This suggests vertical fluxes were mainly controlled by upwelling. Therefore, our result was close to previous studies without consideration of upward diffusion (Wang and Wang, 2007). Upwelling fluxes are accompanied with horizontal displacement, while upward diffusion fluxes stay vertically in the same place. The large overlap of upwelling fluxes and upward diffusion ones results in nutrients in lower layer of the open seas being uplifted to upper layer and the improvement of nutrient structure (Wang and Wang, 2007), which coincides with high primary production areas reported in previous studies (Tian et al., 1993; Chen et al., 2004; Chai et al., 2006; Gong et al., 2006, 2007).

4.3 Characteristics and mechanisms of boundary fluxes

There was no regular pattern for eastern boundary fluxes, seaward in summer but onshore in autumn; onshore for upper layer fluxes but seaward for lower layer fluxes in winter; onshore overall but seaward for lower layer fluxes of DSI and DIP in spring. Eastern boundary fluxes were much smaller than those at other three boundaries for four seasons. Eastern boundary fluxes were 1 to 2 orders of magnitude less than western boundary fluxes in the same season. This is consistent with Huang et al. (2006)'s findings. This suggests that the study area does not likely to export substantial quantities of nutrients to the East China Sea, instead nutrients confined to the coastal region by the complex circulation regime (Zhang et al., 2007a).

Western boundary fluxes flowed into the study area for four seasons, while southern and northern boundary fluxes flowed consistently with the monsoon, with a special case of northern boundary fluxes northward in lower layer in autumn. This is probably because the topographic effect outweighs the shear stress from upper layer. In the same season, southern and northern boundary fluxes were much greater than those at eastern and western boundaries. What is more, southern boundary fluxes (outflow) exceeded northern boundary fluxes (inflow) by one fold in winter, meaning that nutrient flux outflow too rapidly for nutrients to be assimilated by phytoplankton under strong winds. This makes the study area act as a conveyer transferring nutrients from the Yellow Sea to the East China Sea in the whole year.

5 CONCLUSION

A hydrodynamic box model based on ROMS was successfully constructed. Nutrient fluxes in a complex current system were calculated and flux fields were depicted. The major processes controlling the nutrient flux were discussed. The nutrient flux varied greatly in season and space. Water flux outweighs the nutrient concentration in horizontal flux, and upwelling flux outweighs upward diffusion flux in vertical direction (upwelling flux and upward diffusion flux regions overlap all the year). It is found that vertical flux in spring and summer are much greater than that in autumn and winter, and the maximum vertical DIP flux occurs in summer. Additional to the fluxes of CRD, coastal currents, TWC, and the upwelling, nutrient flux inflow from the south Yellow Sea and outflow southward are found crucial to the nutrient budgets of the study area. As a result, Horizontal nutrient flux is controlled by physical dilution and confined to coastal waters and a little into the open seas, and the study area acts as a conveyer transferring nutrients from the Yellow Sea to the East China Sea in the whole year. Vertical nutrient flux in spring and summer is a main source of DIP. Therefore, the hydrodynamic ROMS-based box model is superior to the traditional one in estimating nutrient flux in a complicated hydrodynamic current system and provides a modified box model approach to material flux research.

6 ACKNOWLEDGEMENT

We are grateful to all the participants on the cruises, the captain and the crew.

References

Baretta J W, Ebenhoh W, Ruardij P. 1995. The european-regional-seas-ecosystem-model, a complex marine system model. *Netherlands Journal of Sea Research*, **33**: 233-246.

Barnes H. 1959. Apparatus and Methods of Oceanography. Part 1: Chemical. George Allen and Unwin Ltd, London. 341p.

Blackford J C, Radford P J. 1995. A structure and methodology for marine ecosystem modeling. *Netherlands Journal of Sea Research*, **33**: 247-260.

Camacho-Ibar V F, Carriquiry J D, Smith S V. 2003. Non-

conservative P and N fluxes and net ecosystem production in San Quintin Bay, Mexico. *Estuaries*, **26**: 1 220-1 237.

Chai C, Yu Z, Shen Z, Song X, Cao X, Yao Y. 2009. Nutrient characteristics in the Yangtze River Estuary and the adjacent East China Sea before and after impoundment of the Three Gorges Dam. *Science of the Total Environment*, **407**: 4 687-4 695.

Chai C, Yu Z M, Song X X, Cao X H. 2006. The status and characteristics of eutrophication in the Yangtze River (Changjiang) estuary and the adjacent East China Sea, China. *Hydrobiologia*, **563**: 313-328.

Chang P H, Isobe A. 2003. A numerical study on the Changjiang diluted water in the Yellow and East China Seas. *Journal of Geophysical Research*: *Oceans*, **108**: 1-17.

Chen C T A, Wang S L. 1999. Carbon, alkalinity and nutrient budgets on the East China Sea continental shelf. *Journal of Geophysical Research*, **104**: 20 675-20 620, 20 686.

Chen C. 1996. The Kuroshio intermediate water is the major source of nutrients on the East China Sea continental shelf. *Oceanologica Acta*, **19**: 523-527.

Chen C, Xue P, Ding P, Beardsley R C, Xu Q, Mao X, Gao G, Qi J, Li C, Lin H, Cowles G, Shi M. 2008. Physical mechanisms for the offshore detachment of the Changjiang Diluted Water in the East China Sea. *Journal of Geophysical Research-Oceans*, **113**.

Chen C T A. 1998. Response to Liu's comments on "The Kuroshio Intermediate Water is the major source of nutrients on the East China Sea continental shelf" by Chen (1996). *Oceanologica Acta*, **21**: 713-716.

Chen C T A, Ruo R, Pai S C, Liu C T, Wong G T F. 1995. Exchange of water masses between the East-China-Sea and the Kuroshio off northeastern Taiwan. *Continental Shelf Research*, **15**: 19-39.

Chen H, Yu Z, Yao Q, Mi T, Liu P. 2010. Nutrient concentrations and fluxes in the Changjiang Estuary during summer. *Acta Oceanologica Sinica*, **29**: 107-119.

Chen Y L L, Chen H Y, Gong G C, Lin Y H, Jan S, Takahashi M. 2004. Phytoplankton production during a summer coastal upwelling in the East China Sea. *Continental Shelf Research*, **24**: 1 321-1 338.

Duan S, Liang T, Zhang S, Wang L, Zhang X, Chen X. 2008. Seasonal changes in nitrogen and phosphorus transport in the lower Changjiang River before the construction of the Three Gorges Dam. *Estuarine Coastal and Shelf Scienc*e, **79**: 239-250.

Eigenheer A, Kuhn W, Radach G. 1996. On the sensitivity of ecosystem box model simulations on mixed-layer depth estimates. *Deep-Sea Research Part I*: *Oceanographic Research Papers*, **43**: 1 011-1 027.

Fang T H, Chen J L, Huh C A. 2007. Sedimentary phosphorus species and sedimentation flux in the East China Sea. *Continental Shelf Research*, **27**: 1 465-1 476.

Froelich P N. 1988. Kinetic control of dissolved phosphate in natural rivers and estuaries — a primer on the phosphate buffer mechamism. *Limnology and Oceanography*, **33**: 649-668.

Ganachaud A, Wunsch C. 2002. Oceanic nutrient and oxygen transports and bounds on export production during the World Ocean Circulation Experiment. *Global Biogeochemical Cycles*, **16**.

Gao L, Li D J, Ding P X. 2008. Nutrient budgets averaged over tidal cycles off the Changjiang (Yangtze River) Estuary. *Estuarine Coastal and Shelf Science*, **77**: 331-336.

Gao L, Li D J, Ding P X. 2009. Quasi-simultaneous observation of currents, salinity and nutrients in the Changjiang (Yangtze River) plume on the tidal timescale. *Journal of Marine Systems*, **75**: 265-279.

Gong G C, Chang J, Chiang K P, Hsiung T M, Hung C C, Duan S W, Codispoti L A. 2006. Reduction of primary production and changing of nutrient ratio in the East China Sea: effect of the Three Gorges Dam? *Geophysical Research Letters*, **33**.

Gong G C, Hung C C, Chang J. 2007. Reply to comment by Jinchun Yuan et al. on "Reduction of primary production and changing of nutrient ratio in the East China Sea: Effect of the Three Gorges Dam?". *Geophysical Research Letters*, **34**.

Gordon D C, Boudreau P, Mann K, Ong J, Silvert W, Smith S, Wattayakorn G, Wulff F, Yanagi T. 1996. LOICZ biogeochemical modelling guidelines. LOICZ Core Project, *Netherlands Institute for Sea Research*.

Grasshoff K, Kremling K, Ehrhardt M. 2009. Methods of Seawater Analysis. Verlag Chemie, Weinheim, New York. p.276-281.

Guo X, Miyazawa Y, Yamagata T. 2006. The Kuroshio onshore intrusion along the shelf break of the East China Sea: the origin of the Tsushima Warm Current. *Journal of Physical Oceanography*, **36**: 2 205-2 231.

Guo X, Zhu X H, Wu Q S, Huang D. 2012. The Kuroshio nutrient stream and its temporal variation in the East China Sea. *Journal of Geophysical Research-Oceans*, **117**: C01026.

Hagy J D, III Murrell M C. 2007. Susceptibility of a northern Gulf of Mexico estuary to hypoxia: an analysis using box models. *Estuarine Coastal and Shelf Science*, **74**: 239-253.

Han A, Dai M, Kao S J, Gan J, Li Q, Wang L, Zhai W, Wang L. 2012. Nutrient dynamics and biological consumption in a large continental shelf system under the influence of both a river plume and coastal upwelling. *Limnology and Oceanography*, **57**: 486-502.

Huang Q, Shen H, Wang Z, Liu X, Fu R. 2006. Influences of natural and anthropogenic processes on the nitrogen and phosphorus fluxes of the Yangtze Estuary, China. *Regional Environmental Change*, **6**: 125-131.

Isobe A. 2008. Recent advances in ocean-circulation research on the Yellow Sea and East China Sea shelves. *Journal of Oceanography*, **64**: 569-584.

Kondratyev K Y, Pozdnyakov D V. 1996. Land-ocean interactions in the coastal zone: the LOICZ project. *Nuovo Cimento Della Societa Italiana Di Fisica C —Geophysics and Space Physics*, **19**: 339-354.

Kuhn W, Paetsch J, Thomas H, Borges A V, Schiettecatte L S, Bozec Y, Prowe A E F. 2010. Nitrogen and carbon cycling

in the North Sea and exchange with the North Atlantic-A model study, Part II: carbon budget and fluxes. *Continental Shelf Research*, **30**: 1 701-1 716.

Lee H J, Chao S Y, Liu K K. 2004. Effects of reduced Yangtze River discharge on the circulation of surrounding seas. *Terrestrial Atmospheric and Oceanic Sciences*, **15**: 111-132.

Lenhart H J, Radach G, Backhaus J O, Pohlmann T. 1995. Simulations of the north-sea circulation, its variability, and its implementation as hydrodynamical forcing in ersem. *Netherlands Journal of Sea Research*, **33**: 271-299.

Li M, Xu K, Watanabe M, Chen Z. 2007. Long-term variations in dissolved silicate, nitrogen, and phosphorus flux from the Yangtze River into the East China Sea and impacts on estuarine ecosystem. *Estuarine Coastal and Shelf Science*, **71**: 3-12.

Li X A, Yu Z, Song X, Cao X, Yuan Y. 2011. Nitrogen and phosphorus budgets of the Changjiang River estuary. *Chinese Journal of Oceanology and Limnology*, **29**: 762-774.

Lie H J, Cho C H, Lee J H, Lee S. 2003. Structure and eastward extension of the Changjiang River plume in the East China Sea. *Journal of Geophysical Research-Oceans*, **108**(C3): 3 077.

Liu K K, Tang T Y, Gong G C, Chen L Y, Shiah F K. 2000. Cross-shelf and along-shelf nutrient fluxes derived from flow fields and chemical hydrography observed in the southern East China Sea off northern Taiwan. *Continental Shelf Research*, **20**: 493-523.

Liu S M, Hong G H, Zhang J, Ye X W, Jiang X L. 2009. Nutrient budgets for large Chinese estuaries. *Biogeosciences*, **6**: 2 245-2 263.

Liu X, Shen H. 2001. Estimation of dissolved inorganic nutrients fluxes from the Changjiang River into estuary. *Science in China Series B*: *Chemistry*, **44**: 135-141.

Liu X Q, Yin B S, Hou Y J. 2008a. The dynamic of circulation and temperature-salinity structure in the Changjiang mouth and its adjacent marine area. *Oceanologia et Limnologia Sinica*, 82-89. (in Chinese with English abstract)

Liu X Q, Yin B S, Hou Y J. 2008b. The dynamic of circulation and temperature-salinity structure in the Changjiang mouth and its adjacent marine area II. Major characteristics of the circulation. *Oceanologia et Limnologia Sinica*, 312-320. (in Chinese with English abstract)

Lü X, Qiao F, Xia C, Yuan Y. 2007. Tidally induced upwelling off Yangtze River estuary and in Zhejiang coastal waters in summer. *Science in China Series D-Earth Sciences*, **50**: 462-473.

Lü X, Qiao F, Xia C, Zhu J, Yuan Y. 2006. Upwelling off Yangtze River estuary in summer. *Journal of Geophysical Research-Oceans*, **111**: C11S08.

Ma C F. 2010. Optimization Method and the Matlab Programming. Science Press, Beijing. 264p. (in Chinese with English abstract)

Moll A, Radach G. 2003. Review of three-dimensional ecological modelling related to the North Sea shelf system—Part 1: models and their results. *Progress in Oceanography*, **57**: 175-217.

Nixon S, Oviatt C, Frithsen J, Sullivan B. 1986. Nutrients and the productivity of estuarine and coastal marine ecosystems. *Journal of the Limnological Society of Southern Africa*, **12**: 43-71.

Officer C B. 1980. Box Models Revisited. Estuarine and Wetland Processes. Springer. p.65-114.

Padedda B M, Luglie A, Ceccherelli G, Trebini F, Sechi N. 2010. Nutrient-flux evaluation by the LOICZ Biogeochemical Model in Mediterranean lagoons: the case of Cabras Lagoon (Central-Western Sardinia). *Chemistry and Ecology*, **26**: 147-162.

Paetsch J, Kuehn W. 2008. Nitrogen and carbon cycling in the North Sea and exchange with the North Atlantic—A model study. Part I. Nitrogen budget and fluxes. *Continental Shelf Research*, **28**: 767-787.

Pai S C, Yang C C, P Riley J. 1990. Formation kinetics of the pink azo dye in the determination of nitrite in natural waters. *Analytica Chimica Acta*, **232**: 345-349.

Pei S, Shen Z, Laws E A. 2009. Nutrient dynamics in the upwelling area of Changjiang (Yangtze River) Estuary. *Journal of Coastal Research*, 569-580.

Proctor R, Holt J T, Allen J I, Blackford J. 2003. Nutrient fluxes and budgets for the North West European Shelf from a three-dimensional model. *Science of the Total Environment*, **314**: 769-785.

Radach G, Moll A. 2006. Review of three-dimensional ecological modelling related to the North Sea shelf system. Part II: model validation and data needs. *In*: Gibson R N, Atkinson R J A, Gordon J D M eds. *Oceanography and Marine Biology — an Annual Review*, **44**: 1-60.

Roson G, AlvarezSalgado X A, Perez F F. 1997. A non-stationary box model to determine residual fluxes in a partially mixed estuary, based on both thermohaline properties: application to the Ria de Arousa (NW Spain). *Estuarine Coastal and Shelf Science*, **44**: 249-262.

Schrum C, Alekseeva I, St John M. 2006a. Development of a coupled physical-biological ecosystem model ECOSMO - Part I: Model description and validation for the North Sea. *Journal of Marine Systems*, **61**: 79-99.

Schrum C, St John M, Alekseeva I. 2006b. ECOSMO, a coupled ecosystem model of the North Sea and Baltic Sea: Part II. Spatial-seasonal characteristics in the North Sea as revealed by EOF analysis. *Journal of Marine Systems*, **61**: 100-113.

Shchepetkin A F, McWilliams J C. 2005. The regional oceanic modeling system (ROMS): a split-explicit, free-surface, topography-following-coordinate oceanic model. *Ocean Modelling*, **9**: 347-404.

Shen H T. 2001. Material Flux of the Yangtze River Estuary. Ocean Press, Beijing. 176p.

Shi J Z, Lu L F. 2011. A short note on the dispersion, mixing, stratification and circulation within the plume of the partially-mixed Changjiang River estuary, China. *Journal*

of Hydro-Environment Research, **5**: 111-126.

Simpson J H, Rippeth T P. 1998. Non-conservative nutrient fluxes from budgets for the Irish Sea. *Estuarine Coastal and Shelf Science*, **47**: 707-714.

Strickland J D, Parsons T R. 1968. A Practical Handbook of Seawater Analysis. Fisheries Research Board, Canada. 311p.

Tian R C, Hu F X, Saliot A. 1993. Biogeochemical processes controlling nutrients at the turbidity maximum and the plume water fronts in the Changjiang Estuary. *Biogeochemistry*, **19**: 83-102.

Mao H L, Kan Z J, Lan S F. 1963. A preliminary study of the Yangtze diluted water and its mixing processes. *Oceanologia et Limnologia Sinica*, **3**: 183-207. (in Chinese with English abstract)

Wang B. 2006. Cultural eutrophication in the Changjiang (Yangtze River) plume: history and perspective. *Estuarine Coastal and Shelf Science*, **69**: 471-477.

Wang B, Wang X. 2007. Chemical hydrography of coastal upwelling in the East China Sea. *Chinese Journal of Oceanology and Limnology*, **25**: 16-26.

Wang X, Wang B, Zhang C, Shi X, Zhu C, Xie L, Han X, Xin Y, Wang J. 2008. Nutrient composition and distributions in coastal waters impacted by the Changjiang plume. *Acta Oceanologica Sinica*, **27**: 111-125.

Webster I T, Smith S V, Parslow J S. 2000. Implications of spatial and temporal variation for biogeochemical budgets of estuaries. *Estuaries*, **23**: 341-350.

Wong G T, Chao S Y, Li Y H, Shiah F K. 2000a. The Kuroshio edge exchange processes (KEEP) study — an introduction to hypotheses and highlights. *Continental Shelf Research*, **20**: 335-347.

Wong G T, Li Y H, Chao S Y, Chung Y C. 2000b. Kuroshio Edge Exchange Processes (KEEP)-Interactions between the East China Sea and the Kuroshio. *Continental Shelf Research*, **20**: 4-5.

Yan X H, Jo Y H, Jiang L, Wan Z, Liu W T, Li Y, Zhan J, Du T. 2008. Impact of the Three Gorges Dam water storage on the Yangtze River outflow into the East China Sea. *Geophysical Research Letters*, **35**: L05610.

Zhang J, Liu S M, Ren J L, Wu Y, Zhang G L. 2007a. Nutrient gradients from the eutrophic Changjiang (Yangtze River) Estuary to the oligotrophic Kuroshio waters and re-evaluation of budgets for the East China Sea Shelf. *Progress in Oceanography*, **74**: 449-478.

Zhang L, Liu Z, Zhang J, Hong G H, Park Y, Zhang H F. 2007b. Reevaluation of mixing among multiple water masses in the shelf: an example from the East China Sea. *Continental Shelf Research*, **27**: 1 969-1 979.

Zhang Y, Zhao J P. 2007. The estimationof vertical turbulent diffusivity in the surface layer in the Canada basin. *Periodical of Ocean University of China*, 695-703.

Zhao L, Guo X. 2011. Influence of cross-shelf water transport on nutrients and phytoplankton in the East China Sea: a model study. *Ocean Science*, **7**: 1 405-1 437.

Zhu C C, Kong Y Y, Ding P X. 2008. Experimental study of vertical sediment mixing coefficients in 2D uniform flow. *Journal of East China Normal University* (*Natural Science*), 112-118.

Zhu C C, Kong Y Y, Ding P X. 2009. Vertical diffusion coefficient of suspended sediment inflows. *Journal of Sediment Research*, 43-47.

Zhu J R, Qi D M, Xiao C Y. 2004. Simulated circulations off the Changjiang (Yangtze) River mouth in spring and autumn. *Chinese Journal of Oceanography and Limnol*ogy, **22**: 286-291.

* Appendixes A and B are omitted due to their large-sizes, which can be accessed from http://www.qdio.ac.cn/klmees/2010/web/asp/newsDetail.asp?AutoID=3352.